Diosmin inhibits cell proliferation and induces cell apoptosis through protein phosphatase 2A activation in HA22T human hepatocellular carcinoma cells and blocks tumor growth in xenografted nude mice

Tran Dac Dung[1], Cecilia Hsuan Hsu[2], Truong Van Binh[3], Wei-Wen Kuo[4], Chih-Yang Huang[4]*

[1]School of Clinical Medicine, China Medical University, Taichung, Taiwan
[2]Department of Nursing, MeiHo University, Pingtung, Taiwan
[3]School of Clinical Medicine, Viet Nam Academy of Traditional Medicine, Ha Noi, Viet Nam
[4]Department of Biological Science and Technology, China Medical University, Taichung, Taiwan

P626

2012 The 27th Joint Annual Conference of Biomedical Sciences 第27屆 生物醫學聯合學術年會

Abstract

In this study, we investigated the effect of diosmin on HA22T human hepatocellular carcinoma cell *in vitro* and in an *in vivo* mouse xenograft model. HA22T cells were treated with different concentrations of diosmin and analyzed with MTT assay. Western blot analysis, normal healing flow cytometry, TUNEL, TC-1 staining, RT-PCR, and siRNA transfection assays. Additionally, the HA22T-implanted xenograft nude mice model was applied to confirm the cellular effect. Diosmin showed strong HA22T cell viability inhibition and significantly reduced the cell proliferation proteins as well as induction of cell cycle arrest in the G2/M phase through p53 activation and PI3-Akt-MDM2 signaling pathway inhibition. However, diosmin induced apoptosis, up-regulated death receptor apoptosis pathway markers as well as mitochondrial proteins, and suppressed the survival proteins. PP2A siRNA or okadaic acid reversed the diosmin effect, confirming the role of PP2A in diosmin inhibits cell proliferation and induced HA22T apoptosis. All our experimental evidence indicates that diosmin significantly inhibits cell proliferation and promotes HA22T apoptosis and reduce tumor size in xenograft nude mice via PP2A mediated-dependent manner.

Results

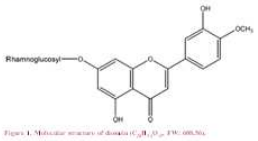

Figure 1. Molecular structure of diosmin ($C_{28}H_{32}O_{15}$, FW: 608.56).

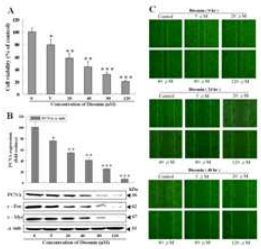

Figure 2. The suppressive effects of diosmin on HA22T cell proliferation.
HA22T cells were incubated with 0, 5, 20, 40, 80, and 120 μM of diosmin for 24 h. (A) Cell viability as measured using MTT assay. (B) Down-regulation of PCNA. α-Tub, and α-Myc proteins expression as revealed by Western blot analysis. α-tubulin was used as a loading control. (C) Cell proliferation was measured using Wound healing analysis at 0 h, 24 h, and 48 h. Photographs indicate relative wound closure as monitored by visual examination using an Olympus phase-contrast microscope. Data are shown as the means ± SD of three independent experiments and denote significant differences from control values with $^{*}p < 0.05$, $^{**}p < 0.01$, and $^{***}p < 0.001$, respectively.

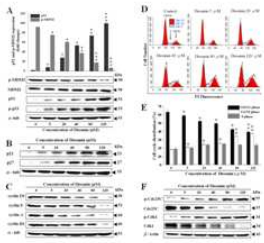

Figure 3. Cell cycle arrest-associated inhibition by diosmin in human hepatocellular carcinoma HA22T cells.
(A) Western blot analysis showing decreased p-RB/RB and increased p53 and p-p53 protein expression. (B) and (C) Cell cycle controlling proteins expression was examined using Western blot with antibodies against proteins as indicated. Equal loads were assessed with an anti-α-tubulin antibody. (D) The cell cycle was determined using flow cytometric analysis. (E) Representative histograms clearly showing a significant diosmin effect on inducing G2 phase cell cycle arrest in HA22T cells. $^{*}p < 0.05$, $^{**}p < 0.01$ versus the control group. (F) Western blot analysis showing decreased Cdc25C, Cdk1, and increased p-Cdc25C and p-Cdk1 protein expression.

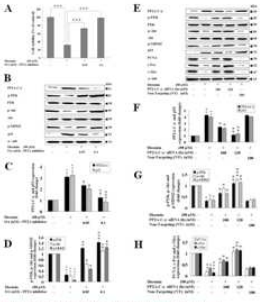

Figure 4. Diosmin inhibits HA22T cell viability through PP2A activation.
HA22T cells were treated with OA, a PP2A inhibitor (0.05 and 0.1 nM for 1 h) or 100 nM and 120 nM PP2A-C α siRNA, a PP2A gene silencer and 100 nM control Non-Targeting (NT) siRNA and then subsequently treated with diosmin (80 μM) for another 24 h. (A) The cell viability was examined using MTT assay. (B) OA inhibits diosmin-induced cell cycle progression by modifying the expression of PP2A-C α, p-PI3K, p-Akt, p-MDM2, and p53 proteins in HA22T cells. (C) siRNA knockdown PP2A-C α to inhibit diosmin-induced HA22T cell apoptosis by Western blot analysis. α-tubulin was used as a loading control. (C and F) Bars represent the relative quantification of PP2A-C α and p53 on the basis of control level. (D and G) Bars represent the relative quantification of p-PI3k, p-Akt, and p-MDM2 based on the control level. (H) Bars represent the relative quantification of PCNA, α-Tub, and α-Myc based on the control level. The quantitative results are expressed as the mean value ± SE ($n = 3$). *, **, and *** denote significant differences from control values with diosmin treatment $p < 0.05$, $p < 0.01$ and $p < 0.001$. #, ## and ### denote significant differences from diosmin treatment of OA or siRNA, $p < 0.05$, $p < 0.01$ and $p < 0.001$, respectively.

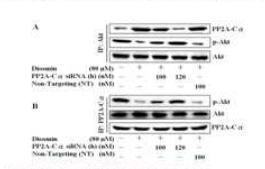

Figure 5. Diosmin activates of PP2A dephosphorylates phosphor-Akt.
(A) Shows the co-immunoprecipitation result regarding the degree of association of Akt with a respective one of PP2A-C α and p-Akt. (B) Shows the co-immunoprecipitation result regarding the degree of association of PP2A-C α with a respective one of p-Akt, and Akt.

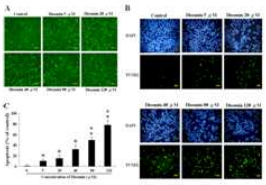

Figure 6. Diosmin induces apoptosis in human HA22T liver cancer cells.
(A) The morphological changes of viable HA22T cells after treatment with diosmin. Photographs were taken on the morphological changes in HA22T cells and then observed under an inverted light microscope. (B) DAPI was used to label nuclei (upper panels) and apoptotic cells nuclei were labelled by TUNEL stain (lower panels). (C) Portions of positive apoptotic cells was based on percentages calculated from three sections of each treatment as described in Materials and Methods.

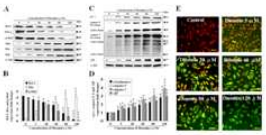

Figure 7. The diosmin effects on some ligand-to-dc pendent apoptotic pathways in human hepatocellular cell line HA22T.
(A) Translocation of the Bcl-2 family proteins by diosmin. (B) Bars represent the relative quantification of Bcl-2, Bax and p-Bad on the basis of control level. (C) The protein expression levels of cytochrome c (cyt c), caspase-9, caspase-3 and apoptosis inducing factor (AIF) were measured by Western blotting. (D) Bars represent the relative quantification of cyt c, caspase-9, caspase-3 and AIF compared to the control. (E) The diosmin effects on the mitochondrial outer membrane permeability of HA22T cells.

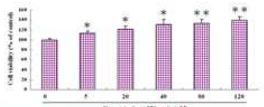

Figure 8. Diosmin shows in no cytotoxic effect on rat primary hepatocytes.
Cells were incubated with 0, 5, 20, 40, 80, and 120 μM diosmin for 24 h. Cell viability was assessed by MTT assay. Data are shown as the means ± SE of three independent experiments and denote significant differences from control values with $^{*}p < 0.05$ and $^{**}p < 0.01$, respectively.

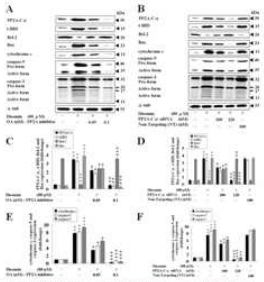

Figure 9. Diosmin induces cell apoptosis through PP2A activation in HA22T cells.
(A) OA blocks diosmin-induced HA22T cell apoptosis by inhibiting the expression of PP2A-C α by Western blot analysis. (B) PP2A-C α siRNA inhibits diosmin-induced HA22T cell apoptosis by Western blot analysis. α-tubulin was used as a loading control. (C and D) Bars represent the relative quantification of PP2A-C α, t-Bid, Bcl-2 and Bax based on control level. (E and F) Bars represent the relative quantification of cyt c, caspase-9 and caspase-3 based on control level.

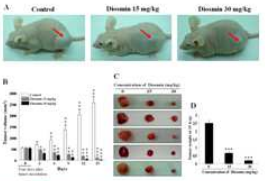

Figure 10. Diosmin effect on the growth of xenografted HA22T tumor tissue in nude mice.
HA22T cells (1×10^6 in 100 μl DMEM) were subcutaneously injected into the left flank of NU/NU mice. Starting at four days after inoculation, when the tumors had reached volume around 800 mm^3, mice were orally treated with diosmin (15 or 30 mg/kg) every day. Tumors of all sacrificed mice 15 days after HA22T inoculation were removed, photographed and weighed. (A) Representative pictures of drug-treated hepatomas. Red arrows indicate tumor mass. (B) Diosmin effect on final tumor volumes. (C) Photographic records of final harvested tumors. (D) Effect of diosmin on final tumor weight. Data were expressed as means ± SE, $n=5$. The statistically significant differences compared with control were calculated by the Student's *t*-test ($^{*}p < 0.05$, $^{**}p < 0.01$ and $^{***}p < 0.001$).

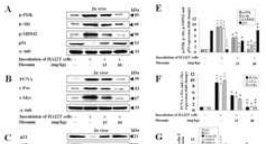

Figure 11. Western blot analysis to different diosmin concentration tumor tissue of HA22T xenograft nude mice model.

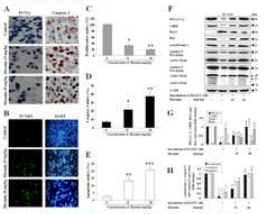

Figure 12. Immunohistochemistry studies and Western blot analysis of tumor tissue treated with different concentrations of diosmin in HA22T xenograft nude mice model.
(A) Representative immunohistochemical staining for PCNA and caspase-3. (B) Representative immunohistochemical staining for TUNEL. (C) The proliferation and (D and E) apoptotic indices were calculated using the ratio of positive cells to total number of tumor cells counted. (F) Western blot analysis of the expression levels of different proteins compared to relative values of controls.

Conclusions

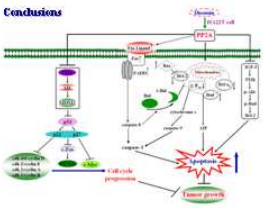

Figure 13. A schematic representation shows the molecular mechanism of diosmin to a potential candidate in vitro for HA22T human cellular carcinoma cell proliferation and promotes apoptosis via PP2A in vitro and in vivo xenografted HA22T tumor growth in the nude mice model.